

CFD Simulation of Crossflow Mixing in a Rod Bundle with Mixing Blades

W. K. In

Korea Atomic Energy Research Institute
P.O. Box 105, Yusong, Taejeon, Korea, 305-600

Abstract

A CFD model was developed in this study to simulate the crossflow mixing in a 4x4 square array rod bundle caused by ripped-open blades. The central subchannel and adjacent subchannels of one grid span were modeled using flow symmetry. The lateral velocity pattern within the central subchannel, lateral velocity and the turbulence intensity in the rod gap region were predicted by the CFD method, and the predictions were compared with the measurements. The CFD simulation shows a vortex flow around the fuel rod caused by a pair of blades, which is consistent with the experimental results. The CFD predictions of the lateral velocity on the mixing sections show a near symmetric profile, but the measurements present an asymmetric velocity profile leading to an inversion of lateral velocity. The predicted mixing rate between the central subchannel and the adjacent subchannels reasonably agrees with the measured one. The CFD prediction shows a parabolic distribution of the RMS velocity but the measured one shows a rather flat distribution near the blade that develops to a parabolic distribution far downstream ($L=29D_o$). The predicted average RMS velocity on a mixing section is also slightly lower than the measured one. This study confirmed that the CFD simulation can present the effect of the ripped-open blades on the crossflow mixing in a rod bundle well.

1. Introduction

The fuel element geometry typically used in nuclear reactors is the rod bundle whose rod-to-rod clearance is maintained by a grid spacer. The heat generated in the rods by the nuclear reaction is removed by the coolant, usually in turbulent flow. The coolant moves axially through the subchannels formed between neighboring fuel rods and between the peripheral fuel rods and the flow tube. One component of a fuel rod bundle is the grid spacer that is to maintain an appropriate rod-to-rod clearance. The fuel spacer affects the coolant flow distribution in a fuel rod bundle, and so spacer geometry has a strong influence on a bundle's thermal-hydraulic characteristics, such as critical heat flux and pressure drop. The flow mixing devices on a grid spacer would enhance the mixing rate

between adjacent subchannels and promote turbulence in the subchannel. The forced mixing effects appeared to be strong near the spacer but were shown to suddenly decay downstream of the spacer. The fuel-grid spacer with flow mixing devices should be therefore designed to maintain the high mixing rate and the turbulence further downstream to improve the DNB performance of fuel-rod bundles without resulting in an excessive pressure drop. It is therefore essential to evaluate the turbulent flow characteristics in detail for the optimal design of a grid spacer with the flow mixing devices. Since the optimal spacer design should consider tremendous shapes and sizes of mixing blades on the grid spacer, the utilization of a CFD method is inevitable to sift the better fuel-spacer designs for the final experimental verification.

The experimental data on flow mixing between the subchannels of bare rod bundles (Rowe *et al.*^[1]; Moller^[2]; Rehme^[3]) showed that the almost periodical flow pulsation between subchannels is the main mechanism for the natural mixing between subchannels resulting from radial pressure gradients between adjacent subchannels. The presence of a grid spacer and flow mixing devices causes the forced mixing of coolant that promotes the flow mixing either within the subchannel or between subchannels. Shen *et al.*^[4] investigated the crossflow mixing effect caused by the grid spacer with the ripped-open blades. They measured the crossflow velocity and the RMS velocity (turbulence intensity) at the rod gap region depending on the angle of a mixing blade on the grid spacer. They obtained the mixing rate depending on the angle of a mixing blade on the grid spacer. Yang and Chung^[5] measured turbulent flow characteristics in subchannels of 5x5 rod bundles with mixing vanes and found that the turbulent mixing and forced mixing occurs behind the grid spacer. Imaizumi *et al.*^[6] developed a CFD method to evaluate 3-D flow characteristics for a PWR fuel assembly in order to improve the design approach. Karoutas *et al.*^[7] performed a 3-D flow analysis for the design of a nuclear fuel spacer by the CFD and experimental methods. Recently, In *et al.*^[8] reported the CFD application to turbulent flow in a rod bundle with mixing blades, and confirmed that the CFD predictions presented 3-D turbulent flow characteristics in the subchannel of a rod bundle with mixing blades well.

This study presents the CFD analysis of the crossflow mixing in a rod bundle with the ripped-open blades on the grid spacer by a CFD code, CFX^[9]. The CFD predictions of the lateral velocity pattern within the central subchannel, the lateral velocity and the turbulence intensity on the rod gap spacing between two adjacent subchannels are compared with the experimental results.

2. CFD Modeling and Analysis

Shen *et al.*^[4] conducted an experiment to improve the understanding of turbulent crossflow processes in rod bundles with promoter (“ripped-open” blades) and to provide the data for developing a computational model of the sweeping flow occurring between adjacent subchannels. The ripped-open mixing blades are arranged symmetrically on the test grid spacer as shown in Fig. 1. The working fluid used in the experiment is water and the temperature and pressure of the water are 20 °C and 0.2 Mpa, respectively. The axial mean velocity of the water in the rod bundle is 2.5 m/s

($Re=14200$). The LDV measurements were performed to obtain data on the distributions of lateral mean velocity and RMS velocity for flow through a 4x4 rod bundle ($P/D=1.375$, $W/D=0.77$, $D=6$ mm) with the ripped-open blades. The blade angle (α) relative to the axial direction of rod was changed to examine the dependence of the mixing rate on the angle of the blade in the experiment.

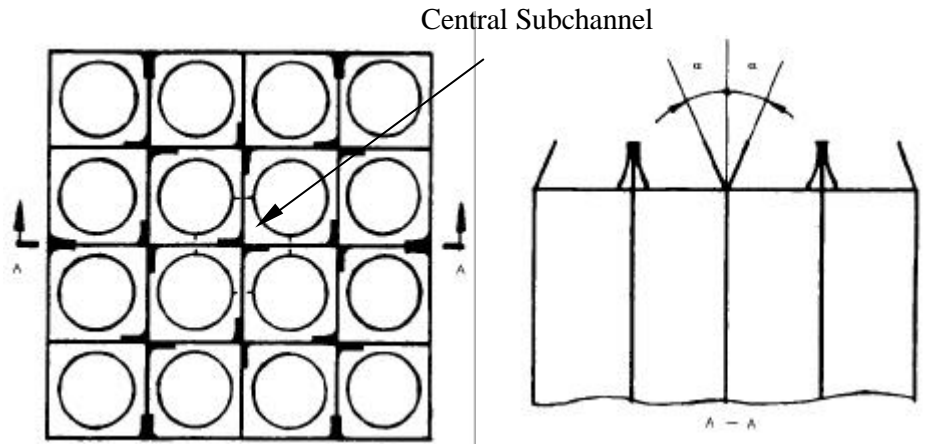


Fig. 1 Layout of a rod bundle and arrangement of ripped-open blades on the grid spacer

The central subchannel and the four neighboring subchannels of one grid span are modeled using flow symmetry as shown in Fig. 2. Special periodic boundary conditions were applied to the side boundaries of the computational domain. The side boundaries with the same letter in Fig. 2 are connected to each other. In other words, what is coming out through one side boundary is going in through another side boundary in the computational model. The spacer strip and blades are treated as infinite thin surfaces in the model, and other fuel spacer elements such as springs and arches are neglected for simplification. This model can simulate the swirl as well as the crossflow mixing caused by the ripped-open blades, but can not predict pressure drop accurately. Since the detailed configuration of the ripped-open blades used in the experiment is unknown, the dimensions of the ripped-open blades were assumed based on engineering judgement. The blade angle is set at 25° from the axial flow direction in this CFD model.

A CFD code, CFX, was used to perform the CFD simulation of the crossflow mixing experiment. The CFD simulation starts 20 mm upstream of the leading edge of the grid spacer and the total length of the CFD model is 545 mm. The inlet boundary conditions used in the simulations were taken from a model without a spacer. Turbulent kinetic energy and turbulent dissipation rate were transferred from the outlet in the no spacer case to the inlet in the simulations with spacers. A uniform velocity of 2.5 m/s was applied to the inlet boundary, and a pressure boundary condition was applied to the outlet boundary with constant pressure in the cross-section.

The computational grid for the central subchannel and the adjacent subchannels is 32x32 cells along the horizontal and vertical centerlines of the computational model (12 cells on the gap spacing), and 238 cells in the axial direction. A non-uniform grid was used to set the fine grid near the blade and the

wall boundary. The standard $k - \epsilon$ turbulence model of Launder and Spalding^[10] was used in this simulation since it is widely used and converges well. A standard under-relaxation method and hybrid difference scheme was used to obtain a converged solution. The calculation was performed on HP9000 C200 (PA8000 CPU, 512 MB RAM) and terminated when the residuals for all governing equations were reduced by a factor of 10^3 to 10^4 . Approximately 4000 to 5000 iterations were needed to obtain a converged solution.

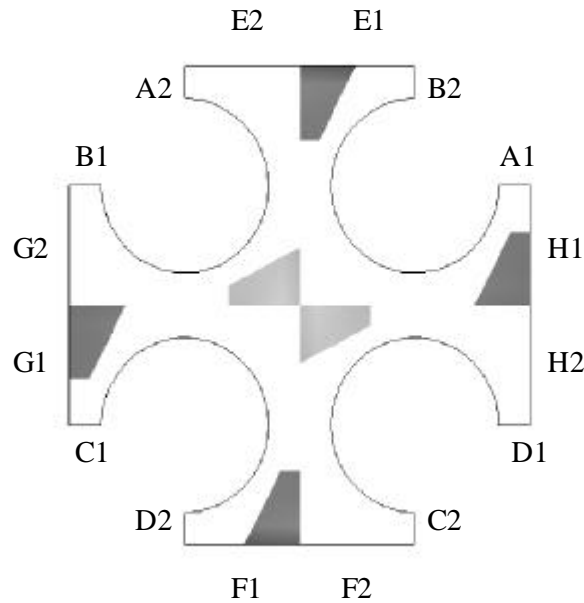


Fig. 2 Cross section of CFD model with periodic side boundaries
(boundaries with the same letter are connected)

3. Results and Discussions

A CFD analysis was conducted to obtain the lateral velocity pattern within the central subchannel, lateral velocity and turbulence intensity on the rod gap spacing between two adjacent subchannels, and the CFD predictions are compared with the experimental results (Shen *et al.*^[4]). Figure 3 shows the comparison of the lateral velocity distributions in two mixing sections (inflow and outflow) at $\alpha = 25^\circ$. The predicted lateral velocity shows almost symmetric profiles, but the measured velocity shows asymmetric profiles near downstream of the spacer. It also shows that the direction of the predicted crossflow does not change in the flow direction, while the measured crossflow changes its direction downstream of the spacer between $L=5D_e$ and $L=10D_e$. This phenomenon is defined as lateral velocity inversion. This is due to the quite different measured velocity nearby two-rod surfaces as shown in Fig. 3(b). The measured velocity is higher at one rod surface and lower at another surface. The experiment also reported somewhat different lateral velocity profiles on the four mixing sections of the central subchannel, but current CFD analysis shows almost the same velocity profiles due to the symmetric arrangement of the ripped-open blades. The magnitude of the predicted lateral velocity agrees

reasonably well with the measured one and slowly decreases in the flow direction.

Figure 4 compares the predicted RMS velocity profiles with the measured ones on two mixing sections downstream. The RMS velocity predictions show a parabolic distribution (lower at the middle of rod gap and higher near the rod surface) due to the parabolic mean velocity profile on the mixing section. However, the measured RMS velocity shows a rather flat distribution near the blade and develops to a parabolic distribution far downstream ($L=29D_o$). The predicted average RMS velocity on a mixing section is also slightly lower than the measured one. This appears to be caused by the quite asymmetry of the mean velocity profile and the lateral velocity inversion in the measurement.

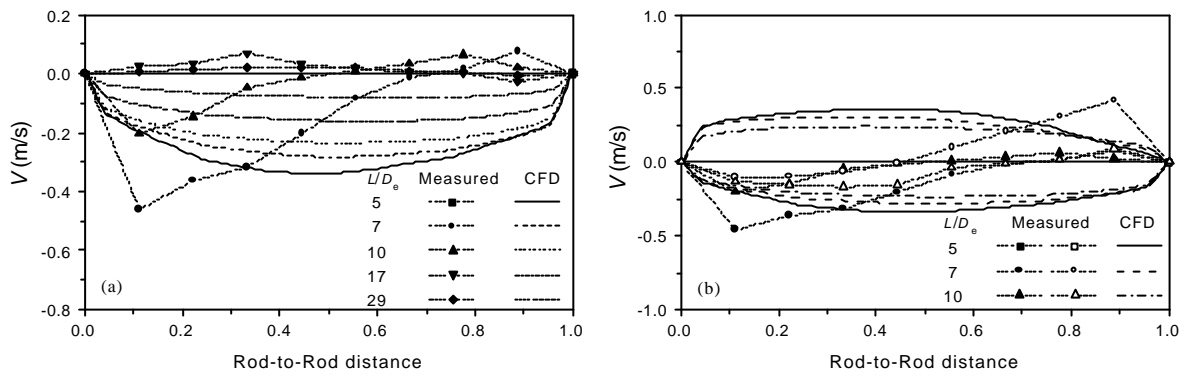


Fig. 3 Comparison of lateral velocity profiles on the crossflow mixing sections;
(a) outflow gap and (b) inflow and outflow gaps

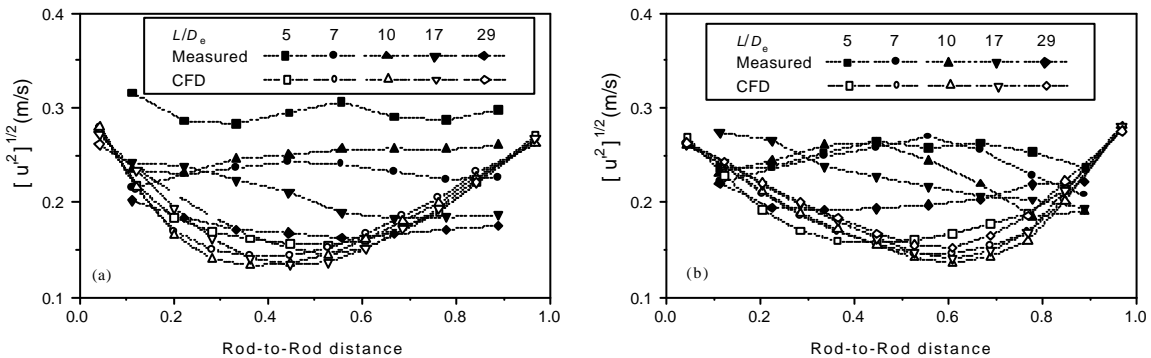
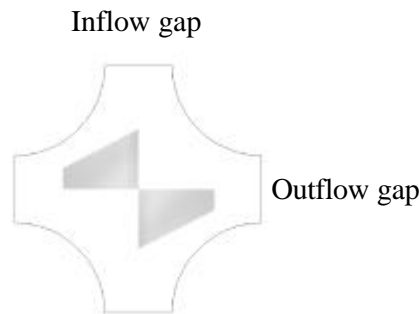


Fig. 4 Comparison of turbulence intensity distributions on the crossflow mixing sections;
(a) inflow gap and (b) outflow gap

Figure 5 shows the predicted and measured lateral velocity patterns on a cross section of the central subchannel downstream at $L=6D_e$ and $L=25D_e$, respectively. Both the predictions and measurements indicate that a pair of ripped-open blades causes largely a crossflow between adjacent subchannels and forms a secondary vortex flow within the subchannel. It can be confirmed that the lateral velocity is higher near the blade and decreases downstream in the flow direction. The predicted and measured lateral velocity at $L=25D_e$ is about 1/3 of that at $L=6D_e$. It is noted that the measured lateral velocity pattern in Fig. 5(a) shows a quite asymmetric crossflow and a cylindrical vortex flow at the center of the subchannel. However, the CFD prediction in Fig. 5(b) shows a symmetric crossflow pattern and appears to form a vortex flow in the quadrants of the subchannel without the blade. The direction of the crossflow velocity changes in the flow direction in the measurement (“lateral velocity inversion”) maintaining the same rotation direction of the vortex in the core, but the both directions keep constant in the prediction. This discrepancy is due to largely the effects of the external wall of the 4x4 array rod bundle and of the inward ripped-open blades installed at the external wall as shown in Fig. 1. The uncertainty in the configuration of the blade in the CFD model would somewhat contribute to the discrepancy.

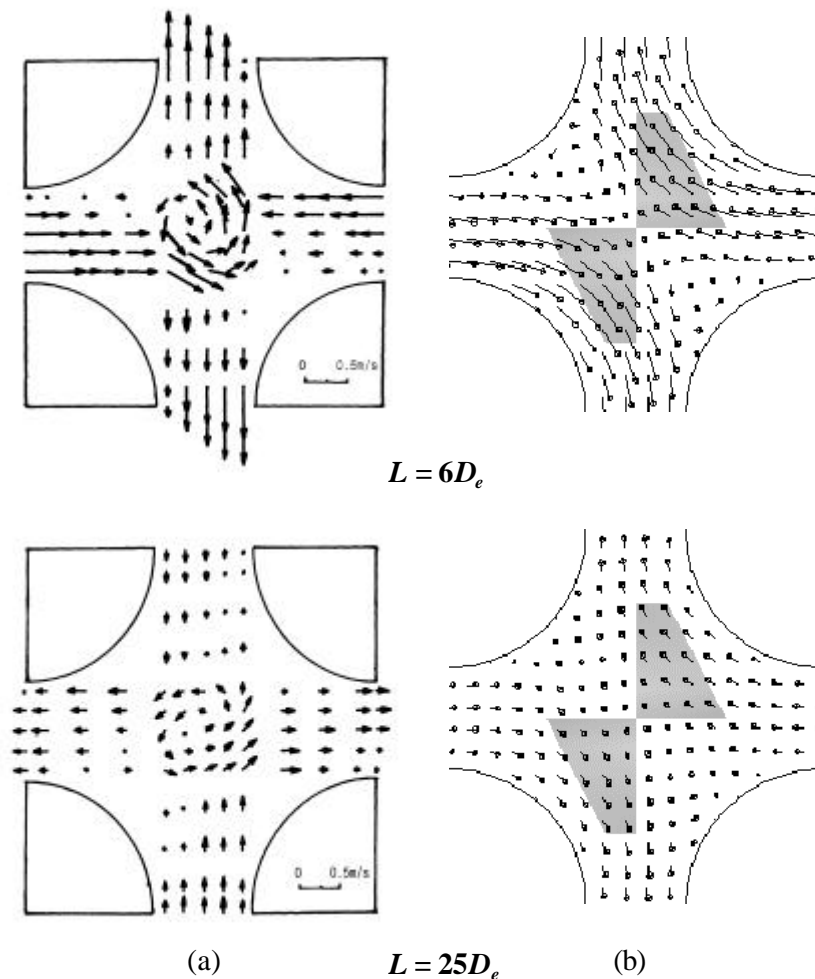


Fig. 5 Comparison of lateral velocity patterns in central subchannel;
 (a) Experiment and (b) CFD prediction

A total mixing rate (Q) is defined as the sum of integration of absolute value of lateral velocity on all four mixing sections per unit length along the rod, i.e.,

$$Q = \int |V| ds. \quad (1)$$

The symbol V is the lateral velocity on each mixing section and s is the rod-to rod gap distance. Figure 6 shows the measured and predicted mixing rates in the flow direction with the blade angle of 25° . The measured mixing rate rapidly decreases and shows one valley in the range of occurrence of the lateral velocity inversion on the mixing sections. The velocity inversion appears to have a considerable influence on the mixing rate. However, the velocity inversion was not predicted in the current CFD prediction as described above, which shows the slow and monotonous decrease of the mixing rate along the axial direction. After the valley of the measured mixing rate ($L/D_e > 17$), the prediction reasonably agrees with the measurement.

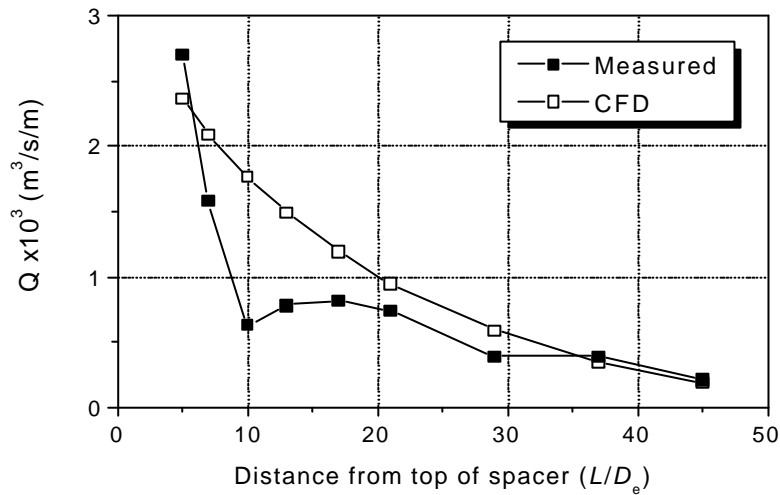


Fig. 6 Axial variation of total crossflow mixing rates in central subchannel

4. Conclusion

An experiment for turbulent flow through a sixteen-rod bundle with the ripped-open blades was simulated in this CFD study. The lateral velocity pattern within central subchannel, lateral velocity and the turbulence intensity in the rod gap region were predicted by the CFD method and the predictions were compared with the measurements. The total crossflow mixing rate in central subchannel in the flow direction was also compared. Consistent with the measurements, the CFD simulation shows a strong crossflow mixing between subchannels and weak vortex flow within the subchannel caused by a pair of blades. The predicted lateral velocity on a mixing section shows near symmetric profile but the measurement results in a quite asymmetric velocity profile leading to an inversion of lateral

velocity. The predicted mixing rate between adjacent subchannels in the flow direction reasonably agrees with the measured one except for the rapid decrease and slight increase (“valley”) in the range of occurrence of the lateral velocity inversion on the mixing sections. The CFD prediction shows a parabolic distribution of the RMS velocity but the measured one shows a rather flat distribution near the blade that develops to a parabolic distribution far downstream ($L=29D_o$). The predicted average RMS velocity on a mixing section is also slightly lower than the measured one. It can be concluded from this study that the CFD simulation can present the effect of the ripped-open blades on the crossflow mixing in a rod bundle well.

Acknowledgements

The authors express their appreciation to the Ministry of Science and Technology (MOST) of Korea for financial support.

References

- [1] Rowe D.S., Johnson B.M. and Knudsen J.G., 1974, “Implications concerning rod bundle crossflow mixing based on measurements of turbulent flow structure,” *Int. J. Heat Mass Transfer*, **17**, 407-419.
- [2] Moller S.V., 1991, “On phenomena of turbulent flow through rod bundles,” *Exp. Thermal and Fluid Science*, **4**, 25-35.
- [3] Rehme K., 1992, “The structure of turbulence in rod bundles and the implications on natural mixing between the subchannels,” *Int. J. Heat Mass Transfer*, **35**, 567-581.
- [4] Shen Y.F., Cao Z.D. and Lu Q.G., 1991, “An investigation of crossflow mixing effect caused by grid spacer with mixing blades in a rod bundle,” *Nucl. Engrg & Des.*, **125**, 111-119.
- [5] Yang S.K. and Chung M.K., 1996, “Spacer grid effects on turbulent flow in rod bundles,” *J. of the Korean Nuclear Science*, **28**, 56-71.
- [6] Imaizumi M., Ichioka T., Hoshi M., Teshima H., Kobayashi H. and Yokoyama T., 1995, “Development of CFD method to evaluate 3-D flow characteristics for PWR fuel assembly,” *Trans. of the 13th Int. Conf. on SMiRT*, Porto Alegre, Brazil, August 13-18.
- [7] Karoutas Z., Gu C.Y. and Scholin B., 1995, “3-D flow analyses for design of nuclear fuel spacer,” *Proc. of the 7th Int. Meeting on Nuclear Reactor Thermal-Hydraulics*, New York, United States, September 10-15.
- [8] In W. K., Chun T. H., Oh D. S. and Jung H. Y., 1998, “CFD application to turbulent flows in rod bundles with mixing blades,” First Korea-Japan Symposium on Nuclear Thermal Hydraulics and Safety, Pusan, Korea, October 21-24.
- [9] AEA Technology (1997), “CFX-4.2 Solver,” Harwell Laboratory, Oxfordshire, UK.
- [10] Launder B.E. and Spalding D.B., 1974, “The numerical computation of turbulent flows,” *Computational Methods in Applied Mechanics and Engineering*, **3**, 269-289.